Available online at www.sciencedirect.com

ScienceDirect

Current Opinion in
Electrochemistry

Review Article

Rational design of carbon-supported single and dual atom catalysts for bifunctional oxygen electrocatalysis

Ting He[1,2], Bingzhe Yu[3], Yi Zhang[2], Xiaoping Ouyang[1] and Shaowei Chen[3]

Abstract

Design and engineering of effective bifunctional electrocatalysts for the oxygen reduction reaction (ORR) and oxygen evolution reaction (OER) represents a critical first step in the further development of rechargeable metal-air batteries, a sustainable energy technology. Recently, nanocomposites based on metal species atomically dispersed within carbon scaffolds have emerged as viable alternatives to the conventional precious metal-based electrocatalysts. In this review, we summarize the latest progress by including a brief introduction to the fundamentals of ORR/OER electrochemistry and an overview of the synthetic strategies and bifunctional performances of carbon-based nanocomposite catalysts with single and dual metal sites. We conclude the review with a perspective about the challenges and opportunities for further innovation of carbon-supported nanocomposites for bifunctional oxygen electrocatalysis.

Addresses

[1] School of Materials Science and Engineering, Xiangtan University, Xiangtan, Hunan 411105, China
[2] Hunan Provincial Key Laboratory of Micro & Nano Materials Interface Science, College of Chemistry and Chemical Engineering, Central South University, Changsha, Hunan 410083, China
[3] Department of Chemistry and Biochemistry, University of California, 1156 High Street, Santa Cruz, CA 95064, United States

Corresponding authors: Chen, Shaowei (shaowei@ucsc.edu); Ouyang, Ouyang (oyxp2003@aliyun.com)

Current Opinion in Electrochemistry 2023, **37:**101197

This review comes from a themed issue on **Energy Storage: Batteries and Supercapacitors**

Edited by **Kenneth Ozoemena**

For a complete overview see the Issue and the Editorial

Available online 10 December 2022

https://doi.org/10.1016/j.coelec.2022.101197

Keywords

Single-atom catalyst, Dual-atom catalyst, Carbon composite, Bifunctional oxygen electrocatalysis, Metal-air battery.

Introduction

Rechargeable metal-air batteries (MABs) have emerged as a sustainable technology for energy conversion and storage, due to the high energy density, low cost, and minimal impacts on the environment; and the performance is mainly determined by the bifunctional activity of the cathode catalysts towards the oxygen reduction reaction (ORR) during discharging and oxygen evolution reaction (OER) during charging [1]. Traditional catalysts are based on noble metals, such as Pt/C for ORR, and RuO_2 or IrO_2 for OER; yet the wide-spread application of MABs has been impeded by the high costs, poor durability and unsatisfactory bifunctional activity of these precious metal-based catalysts [2]. Therefore, it is of fundamental and technological significance to develop high-performance, low-cost bifunctional electrocatalysts for MABs, and nanocomposites based on transition metals atomically dispersed within a nitrogen-doped carbon scaffold have been recognized as viable alternatives, due largely to the formation of unique MN_x coordination moieties [3–5].

Typically, a rechargeable MAB consists of four major components, a metal plate (anode), an aqueous (alkaline) solution or conducting polymer electrolyte, a bifunctional air cathode catalyst, and a membrane separator [6]. In comparison to the theoretical equilibrium potential of 1.65 V, in practice the discharging potential can be as low as 1.3 V and the charging potential as high as over 1.9 V (both at the current density of 10 mA cm^{-2}), mainly due to the sluggish electron-transfer kinetics and complicated pathways of the cathodic ORR/OER processes. In alkaline media, ORR entails three major intermediates, *OOH, *O and *OH, in the following steps,

$$O_2 + * + H_2O + e^- \rightarrow *OOH + OH^- \quad (1)$$

$$*OOH + e^- \rightarrow *O + OH^- \quad (2)$$

$$*O + H_2O + e^- \rightarrow *OH + OH^- \quad (3)$$

$$*OH + e^- \rightarrow OH^- \quad (4)$$

where * stands for active sites. The reaction steps are reversed in OER [6]. To achieve bifunctional activity, it is essential to strike a deliberate balance between the adsorption free energies of these key intermediates onto the active sites. The experimental strategies are primarily based on structural engineering of the metal atomic sites and/or the carbon scaffolds (Scheme 1).

Scheme 1

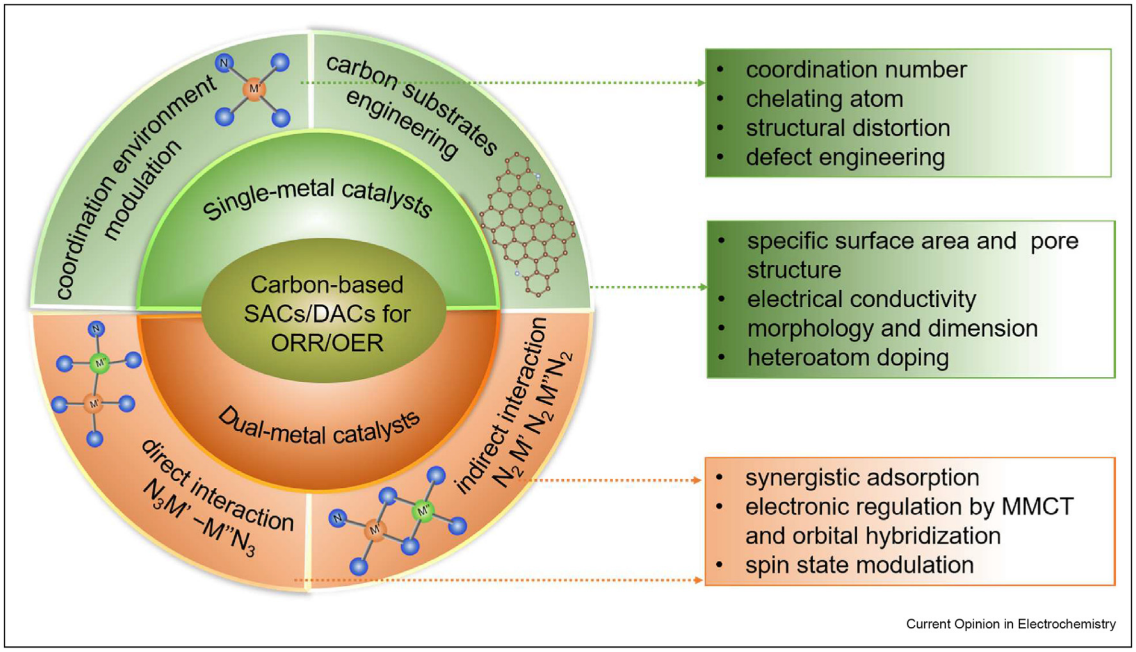

Current Opinion in Electrochemistry

Summary of the mechanistic contributions of carbon-based single and dual atom sites to the ORR/OER electrocatalytic activity.

Herein, we will survey the recent progress in the preparation of carbon-based nanocomposites with single and dual metal sites and their bifunctional performances in rechargeable MABs and conclude the review with a perspective about the challenges and opportunities of carbon-supported nanocomposites as MAB bifunctional oxygen electrocatalysts.

Carbon-based single-metal sites

Modulation of coordination environment

The electronic structure of the single metal sites (i.e., single-atom catalysts, SACs) can be readily regulated by modulating the MN_x atomic configurations (e.g., chelating atoms, coordination number, and structural distortion) as well as defect engineering of the carbon scaffold [7,8]. Among these, MN_4 nanocomposites (e.g., FeN_4, CoN_4, MnN_4, and CuN_4) are of particular interest, with a structure analogous to that of metal phthalocyanine [9–11]. For instance, Yang et al. [12] prepared nanocomposites with CoN_4 moieties dispersed within N-doped graphitic nanosheets (CoN_4/NG) by a surfactant-assisted approach and observed an apparent bifunctional activity with a half-wave potential ($E_{1/2,\,ORR}$) of +0.87 V versus reversible hydrogen electrode (RHE) for ORR and a potential ($E_{10,\,OER}$) of +1.61 V at the current density of 10 mA cm^{-2} for OER. The potential gap (ΔE) between $E_{1/2,ORR}$ and $E_{10,\,OER}$ (0.74 V) was 20 mV lower than that of the commercial Pt/C + IrO_2 counterparts. Chen and coworkers [13] prepared a carbon-based SAC with unique FeN_5 centers by controlled pyrolysis of zeolitic-imidazolate-frameworks-8 (ZIF-8) and graphene oxide. Unlike the plane-like MN_x (x = 2, 3, and 4) sites, tetrahedral FeN_5 moieties exhibit an asymmetric electron depletion zone and can effectively facilitate the generation of reactive intermediates and enhance the eventual catalytic activity with an even lower ΔE of 0.71 V. An asymmetric electronic distribution of the metal centers can also be induced by the incorporation of additional heteroatom dopants, such as S, P, and B [14,15]. For instance, plane-like $FeN_4{-}C$ generally shows a remarkable ORR activity but only a mediocre OER performance [16]; yet additional S doping forming a $FeN_4{-}S$ structure can significantly reduce the OER overpotential by over 100 mV [17]. This is because the additional S doping elevates the charge density, opens the metallic spin channels of the Fe center, and shifts the d-band center towards the Fermi level, leading to moderate OOH* stabilization [18].

Computational studies based on density functional theory (DFT) calculations represent an even more efficient approach to the systematic screening of the MN_x-C nanocomposites as ORR/OER bifunctional catalysts. Recently, Xiao et al. [19] computationally evaluated a series of MN_x-C nanocomposites (M = Mn, Fe, Co, Ni, Cu, Pd, and Pt; and x = 3, 4), as shown in Figure 1a–b. Among the MN_3-C nanocomposites, $NiN_3{-}C$ exhibited the optimal adsorption energy of key intermediates and hence the lowest overpotential (η)

Figure 1

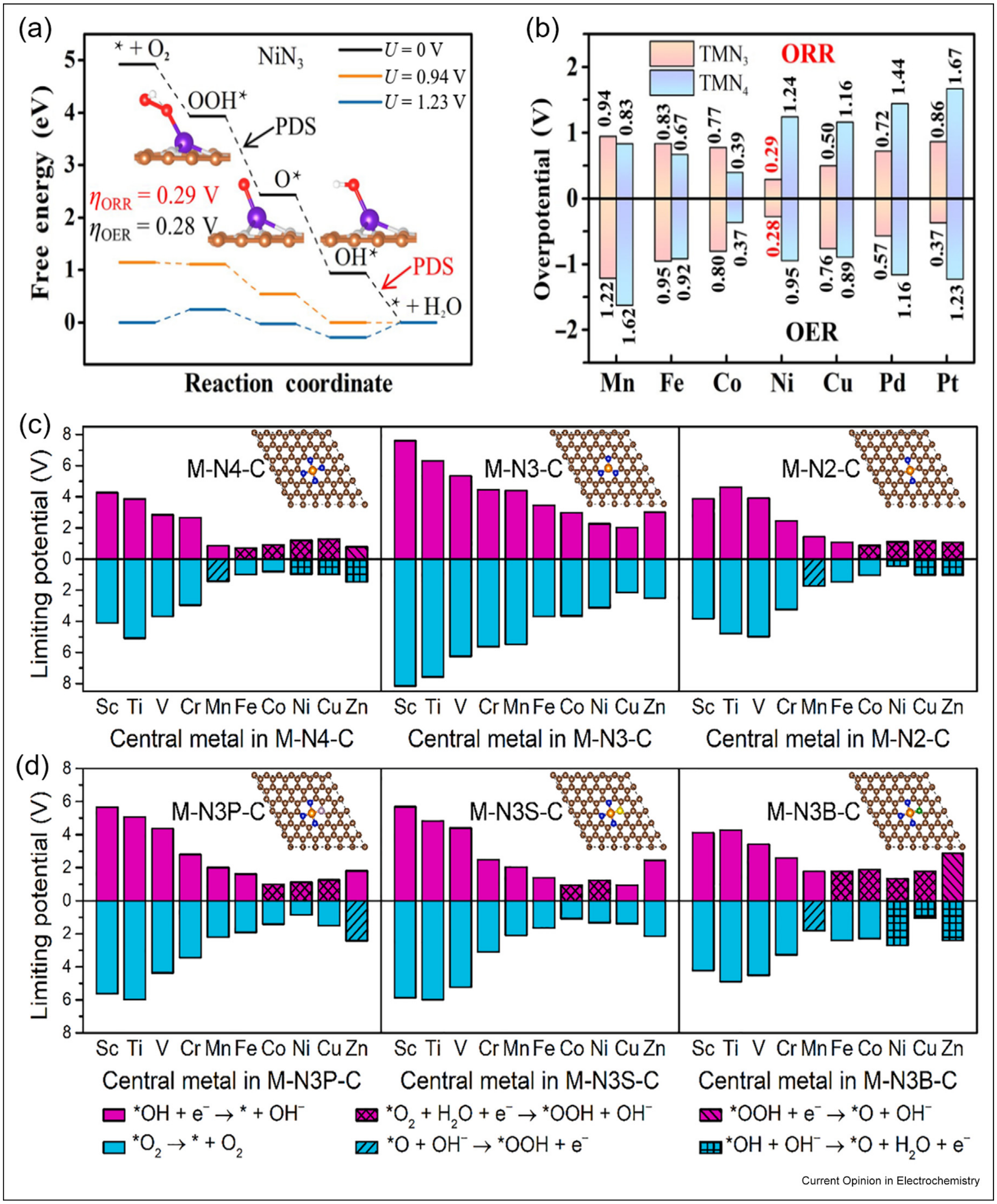

Current Opinion in Electrochemistry

(a) Free energy diagram of NiN_3–C. (b) Overpotentials of ORR and OER for various transition metal-nitrogen (TMN_x) nanocomposites. Reproduced with permission from ref. 19, Copyright 2021, Tsinghua University Press and Springer-Verlag GmbH Germany, part of Springer Nature. (c, d) Limiting potentials of ORR (pink bars) and OER (aqua bars) of six different MN_x-C configurations at +0.402 V vs RHE. Reproduced with permission from ref. 20, Copyright 2021, Elsevier. (For interpretation of the references to color in this figure legend, the reader is referred to the Web version of this article.)

of -0.29 V and $+0.28$ V for ORR and OER, respectively. In contrast, for the MN_4-C series, CoN_4—C displayed the best performance with the overpotentials of -0.39 V for ORR and $+0.37$ V for OER, both subpar as compared to those of NiN_3—C. In another study [20], results from the calculations of 60 different MN_x-C ($x = 4, 3, 2$) and MN_3X—C (X = P, S, and B) moieties show that both the central metal and coordinating atoms strongly impact the performance of oxygen electrocatalysis, predominantly by tuning the adsorption free energy of hydroxyl intermediate (ΔG_{*OH}). From the dual limiting-potential volcano plots for ORR and OER, NiN_2—C was identified as the optimal structure for bifunctional ORR/OER electrocatalysis, followed closely by FeN_4—C, CoN_4—C, CoN_2—C, and NiN_3P—C (Figure 1c—d).

Notably, machine learning (ML) integrated DFT calculations have recently been used to accelerate the design and discovery of SACs through the establishment of deep structure—activity relationships [21,22]. Huang et al. examined a group of 27 C_2N monolayer-supported SACs as promising bifunctional OER/ORR catalysts by theoretical calculations and found a volcano-shaped relationship between the catalytic activity and oxygen adsorption free energy (ΔG_{*O}) [23]. They further unraveled the origin of the element-specific activity by ML modelling based on the random forest algorithm that considers the outer electron number and oxide formation enthalpy as the two most important factors. This model can give an accurate prediction of ΔG_{*O} with much reduced time and cost.

Certainly, to translate these computational advances to practical applications, development of effective synthetic strategies is of urgent need. Several protocols have been developed, such as fixing the coordination number of metal precursors by strong chemical bonds [13], increasing edge sites for unsaturated coordination [24], using metal organic frameworks (MOFs) as the precursors to gain a uniform coordination environment [25], elevating pyrolysis temperature to facilitate the breaking of the metal—N bonds and/or distortion of the geometrical configuration [26,27]. However, due to the complexity of the pyrolysis process, the precise control of the atomic configuration of the metal sites has remained a significant challenge.

Carbon substrate engineering

The electrocatalytic performance can also be aided by the manipulation of the structure of the carbon scaffold, such as the specific surface area, porosity, electrical conductivity, surface morphology, heteroatom doping, among others [28—32]. Because SACs are mostly prepared by a bottom-up method, the metal sites are formed both on the surface and in the interior of the carbon frameworks. A hierarchically porous structure (and hence high specific surface area) can facilitate not only the accessibility of the active sites but also abundant channels for mass transport of electrolyte and reactants [33,34]. Meanwhile, a high degree of graphitization can enhance electron transfer and structural stability by reducing carbon corrosion during electrode reactions. In a recent study [35], biomass hydrogels were utilized as structural templates to prepare carbon aerogels embedded with Fe single atoms by controlled pyrolysis. The resulting composites exhibited a 3D hierarchically porous structure and an excellent ORR/OER electrocatalytic performance with a ΔE of only 0.71 V. Shen et al. [36] prepared graphitic Fe—N—C nanospheres by the pyrolysis of porous polymers synthesized via Schiff base condensation, which exhibited an ultrahigh specific surface area of 1796.0 $m^2\ g^{-1}$, a high degree of graphitization, and a remarkable bifunctional activity and stability. In another study [37], Jiang et al. used a sacrificial template to prepare Co single-atom electrocatalysts with an urchin-like nanotube hierarchical structure derived from ZIF-67 precursors, and the resulting CoN_4—C composites exhibited a remarkable ORR/OER bifunctional activity with a low ΔE of 0.72 V. Hu et al. [38] prepared a nanocomposite of Co single atoms anchored onto N-doped graphene tubes and sheets, where the enrichment of CoN_4 on the graphene tubes facilitated ready access to the ORR active sites, and concurrently the synergistic interactions with the CoN_4-sheet decreased the overpotential of both OER and ORR.

Notably, the structures of both the metal centers and the carbon scaffold are often simultaneously manipulated for the optimization of the catalytic performance. In a recent report [39], Co SACs on ultrathin porous carbon nanosheets were derived from molten salt precursors, where the unique carbon structure facilitated accessibility of the active centers and simultaneously endowed abundant defective CoN_4 configurations. The defects in the second coordination shell of Co SACs promoted the desorption of the OH* intermediate for ORR and facilitated deprotonation of OH* for OER. Nevertheless, excessive carbon defects mean reduced graphitization and compromise electrical conductivity. Thus, a deliberate balance must be struck for an optimal performance.

Carbon-based dual-metal sites

Optimization of the ORR/OER bifunctional activity can also be achieved by the introduction of a second metal site in the proximity into the nanocomposites forming dual-atom catalysts (DACs) [40—45]. For instance, Fe SACs have been known to exhibit a better ORR activity than Ni SACs [46—48], while the OER activity is the opposite [49]. To optimize the ORR/OER bifunctional activity, a step-by-step self-assembly strategy has been developed to prepare Janus hollow graphene with dual-metal atom sites of NiN_4 and FeN_4. Experimental and theoretical studies show that the outer FeN_4 sites and inner NiN_4 sites are respectively active for ORR and OER, and the interconnected metal sites are preferred for the bifunctional activity, in comparison to the independent counterparts [50,51].

Dual-metal sites with direct chemical bonds

For dual-metal sites with a direct chemical bond in a configuration of $N_3M'{-}M''N_3$, the distance between the metal centers is ca. 2.5 Å. This small separation allows for synergistic adsorption of oxygen intermediates; meanwhile, the strong metal–metal charge transfer (MMCT) and orbital hybridization may drastically impact the electronic structures of the metal centers and hence the eventual bifunctional activity [43]. For instance, Hu's group prepared binary Co–Ni sites embedded in N-doped hollow carbon nanocubes by controlled pyrolysis of a dopamine-coated MOF [52]. Theoretical studies demonstrated that the resulting $N_3Co{-}NiN_3$ dual-metal sites synergistically facilitated the adsorption of reaction intermediates and reduced the overall reaction barriers. Zhu et al. [53] fabricated N-doped hollow carbon spheres embedded with $N_3Fe{-}NiN_3$ dual metal sites, and the Fe–Ni bonding interactions manipulated the electronic structures of both the Fe and Ni sites that lowered the energy barriers for ORR and OER (Figure 2a–b). Results from theoretical calculations further showed that the electronically modified Ni and Fe atoms were the active sites for OER and ORR, respectively (Figure 2c–d).

It has also been argued that within the dual-metal atom configuration, a primary site is responsible for the enhanced bifunctional activity, due to the MMCT effects that reduce the reaction energy barrier [54], where the activity of the primary site is electronically modulated by the second one. For instance, Yu et al. [55] synthesized MOF-derived $N_3Fe{-}NiN_3$ DACs embedded in N-doped porous carbon and argued that the Fe site was the active center for the four-electron ORR/OER processes, while the Ni sites helped reduce the energy barrier of the rate-determining step by regulation of the electronic structure of the Fe sites.

Dual-metal sites with indirect interactions

The dual-metal sites can also be connected by indirect interactions, where both metals are in the MN_4 configuration but share two of the four N chelating atoms at a metal–metal distance over 2.6 Å. In a recent DFT study of $N_2M'N_2M''N_2$ DACs (M′, M" = Fe, Co, and Ni) on N-doped graphene (Figure 2e) [56], it was observed that charge transfer still occurred between the two adjacent metal centers and effectively regulated the adsorption energy of key reaction intermediates. Among these, the $N_2FeN_2CoN_2$ DAC stood out as the optimal bifunctional catalysts with the lowest energy barrier for both ORR and OER (Figure 2f), where the Fe–Co interactions not only improved the ORR activity of the Fe sites and OER activity of the Co sites, but also greatly enhanced the ORR activity of the Co sites and OER activity of the Fe sites by changing the OER potential-determining step from the third to the second step. Further mechanistic insights were obtained from *in situ* X-ray absorption spectroscopy (XAS) measurements and theoretical studies [57], where the Ni sites in the DACs preferably underwent structural reconstruction and facilitated the formation of Ni–O–Fe moieties ($N_2FeO_2NiN_2$) as the true dual-metal active sites for OER. The different spin states of Ni and Fe centers led to the formation of spin channels for electron transfer, and optimized the adsorption of key reaction intermediates, resulting in a significantly improved OER activity.

The manipulation of the spin state and hence the catalytic activity of DACs has also been demonstrated in some other studies [58–62]. Li et al. [63] showed that the Fe 3d itinerant charge and moderate spin polarization could be induced by the adjacent Ni atoms, leading to an enhanced catalytic activity. In another study [64], results from DFT calculations show a nearly linear correlation of the energy barriers of key reaction steps in ORR with the Fe magnetic moment. Experimentally, when single Cu sites were incorporated into Fe–N–C aerogels, the Fe centers exhibited a reduced magnetic moment, markedly enhanced ORR activity, and excellent bifunctional activity with an ultralow ΔE of only 0.67 V.

The bifunctional activities of the above catalysts are listed in Table 1, from which one can see that for SACs, the Fe-based ones exhibit the best bifunctional activity. It is well-known that the undesirable Fenton reaction of Fe-based catalysts during the electrocatalytic process can lead to deactivation of the Fe sites and compromise the structural integrity of the nanocomposite catalysts [10,65]. The introduction of a second metal can not only enhance the bifunctional activity, but also greatly improve the stability of the catalyst by suppressing the Fenton reaction. However, in comparison to SACs, the coordination environment of DACs is much more complex, which greatly increases the difficulty of structural characterization and mechanism exploration. Therefore, further research is urgently needed for the establishment of a systematic structure–activity correlation to facilitate the rational design of dual-metal site bifunctional catalysts.

Conclusion and perspectives

In summary, carbon-supported SACs and DACs have emerged as viable bifunctional oxygen electrocatalysts for rechargeable MABs, due to their maximum atom utilization, tunable active sites and well-defined atomic configurations; and the performance can be readily

Figure 2

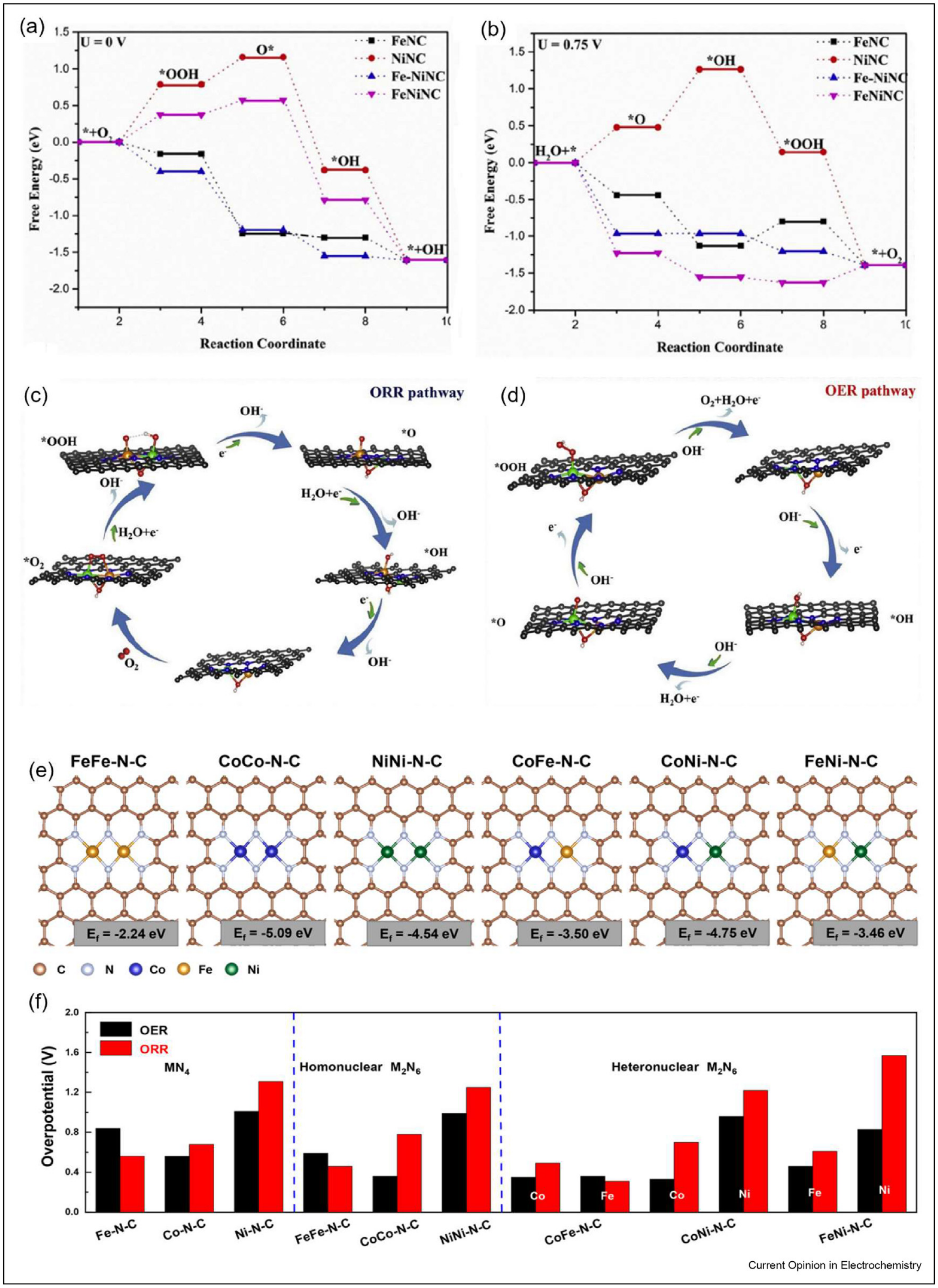

Free energy diagrams of (a) ORR and (b) OER on the $N_3Fe-NiN_3$ dual metal sites, with the proposed pathways shown in (c) and (d), respectively. Reproduced with permission from ref. 53, Copyright 2021, Elsevier. (e) Configurations and formation energies (E_f) of various M_2N_6 models. Brown, silver, yellow, blue, and green spheres indicate the C, N, Fe, Co, and Ni atoms, respectively. (f) Overpotentials of the active sites in all models. Reproduced with permission from ref. 56, Copyright 2022, American Chemical Society. (For interpretation of the references to color in this figure legend, the reader is referred to the Web version of this article.)

Table 1

Bifunctional catalytic performances of carbon-based nanocomposites with single or dual metal sites in alkaline media.

Catalysts	$E_{1/2,ORR}$ (V vs RHE)	$E_{10,OER}$ (V vs RHE)	ΔE (V)	Ref.
CoN$_4$/N-graphitic sheets	+0.87	+1.61	0.74	[12]
FeN$_5$/N-carbon matrix	+0.88	+1.59	0.71	[13]
FeN$_x$/N, S-carbon layer/nanotube	+0.85	+1.60	0.75	[17]
FeN$_x$/N-carbon aerogel	+0.90	+1.60	0.70	[35]
FeN$_5$/N-carbon	+0.91	+1.61	0.70	[36]
CoN$_4$/urchin-like nanotube hierarchical structures	+0.89	+1.61	0.72	[37]
MS−Co SAs−N−C	+0.86	+1.62	0.76	[39]
NiN$_4$−FeN$_4$/hollow graphene nanospheres	+0.83	+1.62	0.79	[50]
CoN$_3$−NiN$_3$/N-carbon nanocube	+0.76	+1.57	0.81	[52]
FeN$_3$−NiN$_3$/N-carbon sphere	+0.84	+1.57	0.73	[53]
FeN$_3$−NiN$_3$N-carbon nanocube	+0.84	+1.50	0.66	[55]
CoN$_4$−FeN$_4$/N-graphene	+0.90	+1.59	0.69	[56]
FeN$_4$−NiN$_4$/N-carbon	+0.86	+1.55	0.69	[63]
FeN$_4$−CuN$_4$/N-carbon aerogel	+0.94	+1.61	0.67	[64]

manipulated by structural engineering of the metal atomic configurations as well as the carbon scaffolds. Yet, despite substantial progress in recent research, further studies are strongly desired for further enhancement of the electrocatalytic activity. This mainly involves the following issues, precise regulation of the coordination configurations of the metal centers, interactions between the metal centers, and optimization of the structure of the carbon scaffolds.

First, carbon-based SACs and DACs synthesized by pyrolysis at high temperatures are usually composed of a mixture of metal sites in a wide range of coordination configurations that may exhibit a widely different electrocatalytic activity. This renders it challenging to correlate the material structure with the electrocatalytic performance and unravel the actual active sites. Development of effective strategies to precisely control the coordination environment of the metal sites is highly desired.

Second, the catalytic active centers may entail a dynamic evolution during electrochemical reactions. In situ and even operando characterization of the nanocomposite catalysts is anticipated to yield important insights into the identification of the actual active sites/configurations.

Third, the stability during the electrode reaction is a key factor in practical applications. During long-term charge−discharge cycles at high potentials, carbon-based nanocomposites are known to exhibit apparent degradation, due to demetallation, carbon oxidation and bulk carbon corrosion. Therefore, strategies are urgently needed to enhance the structural stability of the nanocomposite catalysts by, for instance, increasing the fraction of highly stable metal sites [66], improving the antioxidation of the metal centers [67], and developing advanced carbon substrates with both high graphitization and abundant defects to support the metal sites.

Declaration of competing interest

The authors declare that they have no known competing financial interests or personal relationships that could have appeared to influence the work reported in this paper.

Data availability

Data will be made available on request.

Acknowledgments

This work was supported, in part, by the National Science Foundation (CHE-1900235 and CHE-2003685). Y. Z. acknowledges support from the National Natural Science Foundation of China (21972169, 21773311) and Hunan Provincial Science and Technology Plan Project (2019TP1001). T. H. thanks the Postdoctoral Research Foundation of Central South University (140050038) and Xiangtan University Scientific Research Project Funding (KZ0808469).

References

Papers of particular interest, published within the period of review, have been highlighted as:

* of special interest
* * of outstanding interest

1. Wei Q, Fu Y, Zhang G, Sun S: **Rational design of carbon-based oxygen electrocatalysts for zinc−air batteries**. *Curr. Opin. Electrochem.* 2017, **4**:45−59. https://www.sciencedirect.com/science/article/pii/S2451910317301096.

2. Zeng K, Zheng X, Li C, Yan J, Tian J-H, Jin C, Strasser P, Yang R: **Recent advances in non-noble bifunctional oxygen electrocatalysts toward large-scale production**. *Adv Funct Mater* 2020, **30**, 2000503. https://onlinelibrary.wiley.com/doi/abs/10.1002/adfm.202000503.

3. Peng Y, Lu B, Chen S: **Carbon-supported single atom catalysts for electrochemical energy conversion and storage**. *Adv Mater* 2018, **30**, 1801995. https://onlinelibrary.wiley.com/doi/abs/10.1002/adma.201801995.

4. Zhao S, Yin H, Xia H, Qu G, Yi S, Pang H, Yan W, Zhang J, Mu S: **The assembling principle and strategies of high-density**

atomically dispersed catalysts. *Chem Eng J* 2021, **417**, 127917. https://www.sciencedirect.com/science/article/pii/S1385894720340365.

5. Zang W, Kou Z, Pennycook SJ, Wang J: **Heterogeneous single atom electrocatalysis, where "singles" are "married."**. *Adv Mater* 2020, **10**, 1903181. https://onlinelibrary.wiley.com/doi/abs/10.1002/aenm.201903181.
6. Haruna AB, Ozoemena KI: **Manganese-based bifunctional electrocatalysts for zinc-air batteries**. *Curr. Opin. Electrochem.* 2020, **21**:219−224. https://www.sciencedirect.com/science/article/pii/S2451910320300521.
7. Lu B, Liu Q, Chen S: **Electrocatalysis of single-atom sites: impacts of atomic coordination**. *ACS Catal* 2020, **10**: 7584−7618, https://doi.org/10.1021/acscatal.0c01950.
8. Yuan Y, Zhang Q, Yang L, Wang L, Shi W, Liu P, Gao R, Zheng L, Chen Z, Bai Z: **Facet strain strategy of atomically dispersed Fe-N-C catalyst for efficient oxygen electrocatalysis**. *Adv Funct Mater* 2022, **32**, 2206081. https://onlinelibrary.wiley.com/doi/abs/10.1002/adfm.202206081.
9. Vasudevan P, Santosh, Mann N, Tyagi S: **Transition metal complexes of porphyrins and phthalocyanines as electrocatalysts for dioxygen reduction**. *Transit Met. Chem.* 1990, **15**: 81−90, https://doi.org/10.1007/BF01023892.
10. Li J, Chen M, Cullen DA, Hwang S, Wang M, Li B, Liu K, Karakalos S, Lucero M, Zhang H, Lei C, *et al.*: **Atomically dispersed manganese catalysts for oxygen reduction in proton-exchange membrane fuel cells**. *Nat Catal* 2018, **1**: 935−945, https://doi.org/10.1038/s41929-018-0164-8.
11. Chen Y, Ji S, Wang Y, Dong J, Chen W, Li Z, Shen R, Zheng L, Zhuang Z, Wang D, Li Y: **Isolated single iron atoms anchored on N-doped porous carbon as an efficient electrocatalyst for the oxygen reduction reaction**. *Angew Chem Int Ed* 2017, **56**: 6937−6941, https://doi.org/10.1002/anie.201702473.
12. Yang L, Shi L, Wang D, Lv Y, Cao D: **Single-atom cobalt electrocatalysts for foldable solid-state Zn-air battery**. *Nano Energy* 2018, **50**:691−698. https://www.sciencedirect.com/science/article/pii/S221128551830418X.
13. Li L, Chen Y-J, Xing H-R, Li N, Xia J-W, Qian X-Y, Xu H, Li W-Z, Yin F-X, He G-Y, Chen H-Q: **Single-atom Fe-N$_5$ catalyst for high-performance zinc-air batteries**. *Nano Res* 2022, **15**, https://doi.org/10.1007/s12274-022-4424-1.
14. Wang M, Cao L, Du X, Zhang Y, Jin F, Zhang M, Li Z, Su K: **Highly dispersed Co-, N-, S-doped topological defect-rich hollow carbon nanoboxes as superior bifunctional oxygen electrocatalysts for rechargeable Zn−air batteries**. *ACS Appl Mater Interfaces* 2022, **14**:25427−25438, https://doi.org/10.1021/acsami.2c04030.
15. Shang H, Zhou X, Dong J, Li A, Zhao X, Liu Q, Lin Y, Pei J, Li Z, Jiang Z: **Engineering unsymmetrically coordinated Cu-S$_1$N$_3$ single atom sites with enhanced oxygen reduction activity**. *Nat Commun* 2020, **11**:1−11. https://www.nature.com/articles/s41467-020-16848-8.
16. Wan W, Triana CA, Lan J, Li J, Allen CS, Zhao Y, Iannuzzi M, Patzke GR: **Bifunctional single atom electrocatalysts: coordination−performance correlations and reaction pathways**. *ACS Nano* 2020, **14**:13279−13293, https://doi.org/10.1021/acsnano.0c05088.
17. Chen P, Zhou T, Xing L, Xu K, Tong Y, Xie H, Zhang L, Yan W, Chu W, Wu C: **Atomically dispersed iron−nitrogen species as electrocatalysts for bifunctional oxygen evolution and reduction reactions**. *Angew Chem Int Ed* 2017, **129**:625−629. https://onlinelibrary.wiley.com/doi/full/10.1002/ange.201610119.
18. Zhang X, Zhang Q, Cui J, Yan J, Liu J, Wu Y: **New insights into the key bifunctional role of sulfur in Fe−N−C single-atom catalysts for ORR/OER**. *Nanoscale* 2022, **14**:3212−3223, https://doi.org/10.1039/D1NR07851H.
19. ** Xiao G, Lu R, Liu J, Liao X, Wang Z, Zhao Y: **Coordination environments tune the activity of oxygen catalysis on single atom catalysts: a computational study**. *Nano Res* 2022, **15**: 3073−3081, https://doi.org/10.1007/s12274-021-3964-0.

This work computationally evaluates a series of MN$_x$-C composites (M = Mn, Fe, Co, Ni, Cu, Pd, and Pt; and x = 3, 4) and shows that NiN$_3$−C exhibits the optimal adsorption energy of key intermediates.

20. ** Liu J, Xiao J, Luo B, Tian E, Waterhouse GIN: **Central metal and ligand effects on oxygen electrocatalysis over 3d transition metal single-atom catalysts: a theoretical investigation**. *Chem Eng J* 2022, **427**, 132038. https://www.sciencedirect.com/science/article/pii/S1385894721036172.

The authors systematically examine 60 different MN$_x$-C (x = 4, 3, 2 and MN$_3$X−C (X = P, S, and B) moieties by DFT calculations, and conclude that the performance of oxygen electrocatalysis is tuned predominantly by the adsorption free energy of hydroxyl intermediate.

21. Wu L, Guo T, Li T: **Machine learning-accelerated prediction of overpotential of oxygen evolution reaction of single-atom catalysts**. *iScience* 2021, **24**, 102398. https://www.sciencedirect.com/science/article/pii/S2589004221003667.
22. Tamtaji M, Gao H, Hossain MD, Galligan PR, Wong H, Liu Z, Liu H, Cai Y, Goddard WA, Luo Z: **Machine learning for design principles for single atom catalysts towards electrochemical reactions**. *J Mater Chem A* 2022, **10**:15309−15331, https://doi.org/10.1039/D2TA02039D.
23. Ying Y, Fan K, Luo X, Qiao J, Huang H: **Unravelling the origin of bifunctional OER/ORR activity for single-atom catalysts supported on C$_2$N by DFT and machine learning**. *J Mater Chem A* 2021, **9**:16860−16867, https://doi.org/10.1039/D1TA04256D.
24. Liu J, Gong Z, Allen C, Ge W, Gong H, Liao J, Liu J, Huang K, Yan M, Liu R, He G, *et al.*: **Edge-hosted Fe-N$_3$ sites on a multiscale porous carbon framework combining high intrinsic activity with efficient mass transport for oxygen reduction**. *Chem Catal* 2021, **1**:1291−1307. https://www.sciencedirect.com/science/article/pii/S2667109321002347.
25. Song Z, Zhang L, Doyle-Davis K, Fu X, Luo J-L, Sun X: **Recent advances in MOF-derived single atom catalysts for electrochemical applications**. *Adv Energy Mater* 2020, **10**, 2001561. https://onlinelibrary.wiley.com/doi/abs/10.1002/aenm.202001561.
26. He YH, Shi QR, Shan WT, Li X, Kropf AJ, Wegener EC, Wright J, Karakalos S, Su D, Cullen DA, Wang GF, *et al.*: **Dynamically unveiling metal−nitrogen coordination during thermal activation to design high-efficient atomically dispersed CoN$_4$ active sites**. *Angew Chem Int Ed* 2021, **133**:9602−9612. https://onlinelibrary.wiley.com/doi/full/10.1002/anie.202017288.
27. Li JZ, Zhang HG, Samarakoon W, Shan WT, Cullen DA, Karakalos S, Chen MJ, Gu DM, More KL, Wang GF, Feng ZX, *et al.*: **Thermally driven structure and performance evolution of atomically dispersed FeN$_4$ sites for oxygen reduction**. *Angew Chem Int Ed* 2019, **131**:19147−19156. https://onlinelibrary.wiley.com/doi/full/10.1002/ange.201909312.
28. Kim K, Kang T, Kim M, Kim J: **Three-dimensional entangled and twisted structures of nitrogen doped poly-(1,4-diethynylbenzene) chain combined with cobalt single atom as a highly efficient bifunctional electrocatalyst**. *Appl. Catal. B* 2020, **275**, 119107. https://www.sciencedirect.com/science/article/pii/S0926337320305221.
29. Zang W, Sumboja A, Ma Y, Zhang H, Wu Y, Wu S, Wu H, Liu Z, Guan C, Wang J, Pennycook SJ: **Single Co atoms anchored in porous N-doped carbon for efficient Zinc−Air battery cathodes**. *ACS Catal* 2018, **8**:8961−8969, https://doi.org/10.1021/acscatal.8b02556.
30. Zhong L, Jiang C, Zheng M, Peng X, Liu T, Xi S, Chi X, Zhang Q, Gu L, Zhang S, Shi G, *et al.*: **Wood carbon based single-atom catalyst for rechargeable Zn−air batteries**. *ACS Energy Lett* 2021, **6**:3624−3633, https://doi.org/10.1021/acsenergylett.1c01678.
31. Peng L, Shang L, Zhang T, Waterhouse GIN: **Recent advances in the development of single-atom catalysts for oxygen electrocatalysis and zinc−air batteries**. *Adv Energy Mater* 2020, **10**, 2003018. https://onlinelibrary.wiley.com/doi/abs/10.1002/aenm.202003018.

32. Mercado R, Wahl C, En Lu J, Zhang T, Lu B, Zhang P, Lu JQ, Allen AL, Zhang JZ, Chen S: **Nitrogen-doped porous carbon cages for electrocatalytic reduction of oxygen: enhanced performance with iron and cobalt dual metal centers**. *ChemCatChem* 2020, **12**:3230–3239. https://chemistry-europe.onlinelibrary.wiley.com/doi/abs/10.1002/cctc.201902324.

33. Wan C, Duan X, Huang Y: **Molecular design of single-atom catalysts for oxygen reduction reaction**. *Adv Energy Mater* 2020, **10**, 1903815. https://onlinelibrary.wiley.com/doi/abs/10.1002/aenm.201903815.

34. Wagh NK, Shinde SS, Lee CH, Jung J-Y, Kim D-H, Kim S-H, Lin C, Lee SU, Lee J-H: **Densely colonized isolated Cu-N single sites for efficient bifunctional electrocatalysts and rechargeable advanced Zn-air batteries**. *Appl. Catal. B* 2020, **268**, 118746. https://www.sciencedirect.com/science/article/pii/S0926337320301612.

35. He T, Lu B, Chen Y, Wang Y, Zhang Y, Davenport JL, Chen AP, Pao C-W, Liu M, Sun Z: **Nanowrinkled carbon aerogels embedded with FeN$_x$ sites as effective oxygen electrodes for rechargeable zinc-air battery**. *Research* 2019, **2019**, 6813585, https://doi.org/10.34133/2019/6813585.

36. Lyu D, Mollamahale YB, Huang S, Zhu P, Zhang X, Du Y, Wang S, Qing M, Tian ZQ, Shen PK: **Ultra-high surface area graphitic Fe-N-C nanospheres with single-atom iron sites as highly efficient non-precious metal bifunctional catalysts towards oxygen redox reactions**. *J Catal* 2018, **368**:279–290. https://www.sciencedirect.com/science/article/pii/S0021951718304093.

37. Sun X, Sun S, Gu S, Liang Z, Zhang J, Yang Y, Deng Z, Wei P, Peng J, Xu Y, Fang C, *et al.*: **High-performance single atom bifunctional oxygen catalysts derived from ZIF-67 superstructures**. *Nano Energy* 2019, **61**:245–250. https://www.sciencedirect.com/science/article/pii/S2211285519303775.

38. * Ban J, Wen X, Xu H, Wang Z, Liu X, Cao G, Shao G, Hu J: **Dual evolution in defect and morphology of single-atom dispersed carbon based oxygen electrocatalyst**. *Adv Funct Mater* 2021, **31**, 2010472, https://doi.org/10.1002/adfm.202010472.

A hybrid structure of CoN$_4$ sites supported on graphene tubes/sheets is derived from the ZnCo-ZIF in the presence of dicyandiamide. The enrichment of CoN$_4$ on the graphene tubes not only facilitates the oxygen reaction pathway, but also synergizes with the CoN$_4$-sheets to decrease the overpotentials of OER and ORR.

39. Wang K, Lu Z, Lei J, Liu Z, Li Y, Cao Y: **Modulation of ligand fields in a single-atom site by the molten salt strategy for enhanced oxygen bifunctional activity for zinc-air batteries**. *ACS Nano* 2022, **16**, https://doi.org/10.1021/acsnano.2c01748.

40. Li X, Duan S, Sharman E, Zhao Y, Yang L, Zhuo Z, Cui P, Jiang J, Luo Y: **Exceeding the volcano relationship in oxygen reduction/evolution reactions using single-atom-based catalysts with dual-active-sites**. *J Mater Chem A* 2020, **8**:10193–10198, https://doi.org/10.1039/D0TA01399D.

41. Chen Y, Hu S, Nichols F, Bridges F, Kan S, He T, Zhang Y, Chen S: **Carbon aerogels with atomic dispersion of binary iron–cobalt sites as effective oxygen catalysts for flexible zinc–air batteries**. *J Mater Chem A* 2020, **8**:11649–11655, https://doi.org/10.1039/D0TA04633G.

42. Chen C, Cheng D, Liu S, Wang Z, Hu M, Zhou K: **Engineering the multiscale structure of bifunctional oxygen electrocatalyst for highly efficient and ultrastable zinc-air battery**. *Energy Storage Mater* 2020, **24**:402–411. https://www.sciencedirect.com/science/article/pii/S2405829719308888.

43. Cui T, Wang Y-P, Ye T, Wu J, Chen Z, Li J, Lei Y, Wang D, Li Y: **Engineering dual single-atom sites on 2D ultrathin N-doped carbon nanosheets attaining ultra-low-temperature zinc-air battery**. *Angew Chem Int Ed* 2022, **61**, e202115219, https://doi.org/10.1002/anie.202115219.

44. Zhao X, Liu X, Huang B, Wang P, Pei Y: **Hydroxyl group modification improves the electrocatalytic ORR and OER activity of graphene supported single and bi-metal atomic catalysts (Ni, Co, and Fe)**. *J Mater Chem A* 2019, **7**:24583–24593, https://doi.org/10.1039/C9TA08661G.

45. Zhang J, Huang Q-a, Wang J, Wang J, Zhang J, Zhao Y: **Supported dual-atom catalysts: preparation, characterization, and potential applications**. *Chin J Catal* 2020, **41**:783–798. https://www.sciencedirect.com/science/article/pii/S1872206720635367.

46. Peng H, Liu F, Liu X, Liao S, You C, Tian X, Nan H, Luo F, Song H, Fu Z, Huang P: **Effect of transition metals on the structure and performance of the doped carbon catalysts derived from polyaniline and melamine for ORR application**. *ACS Catal* 2014, **4**:3797–3805, https://doi.org/10.1021/cs500744x.

47. Kattel S, Wang G: **A density functional theory study of oxygen reduction reaction on Me–N$_4$ (Me = Fe, Co, or Ni) clusters between graphitic pores**. *J Mater Chem A* 2013, **1**: 10790–10797, https://doi.org/10.1039/C3TA12142A.

48. Mercado R, Nichols F, Chen S: **Nitrogen-doped carbon flowers with Fe and Ni dual metal centers for effective electroreduction of oxygen**. *Inorganics* 2022, **10**:36. https://www.mdpi.com/2304-6740/10/3/36.

49. Fei H, Dong J, Feng Y, Allen CS, Wan C, Volosskiy B, Li M, Zhao Z, Wang Y, Sun H, An P, *et al.*: **General synthesis and definitive structural identification of MN$_4$C$_4$ single-atom catalysts with tunable electrocatalytic activities**. *Nat. Catal.* 2018, **1**:63–72, https://doi.org/10.1038/s41929-017-0008-y.

50. * Chen J, Li H, Fan C, Meng Q, Tang Y, Qiu X, Fu G, Ma T: **Dual single-atomic Ni-N$_4$ and Fe-N$_4$ sites constructing Janus hollow graphene for selective oxygen electrocatalysis**. *Adv Mater* 2020, **32**, 2003134, https://doi.org/10.1002/adma.202003134.

A Janus NiN$_4$/FeN$_4$ electrocatalyst is prepared through an effective step-by-step self-assembly strategy, where the FeN$_4$ sites make dominant contributions to the ORR activity, while the NiN$_4$ sites are responsible for the OER activity. This results in excellent electrocatalytic selectivity and bifunctionality.

51. Ma Y, Fan H, Wu C, Zhang M, Yu J, Song L, Li K, He J: **An efficient dual-metal single-atom catalyst for bifunctional catalysis in zinc-air batteries**. *Carbon* 2021, **185**:526–535. https://www.sciencedirect.com/science/article/pii/S0008622321009350.

52. Han X, Ling X, Yu D, Xie D, Li L, Peng S, Zhong C, Zhao N, Deng Y, Hu W: **Atomically dispersed binary Co-Ni sites in nitrogen-doped hollow carbon nanocubes for reversible oxygen reduction and evolution**. *Adv Mater* 2019, **31**, 1905622. https://onlinelibrary.wiley.com/doi/abs/10.1002/adma.201905622.

53. ** Zhu X, Zhang D, Chen C-J, Zhang Q, Liu R-S, Xia Z, Dai L, Amal R, Lu X: **Harnessing the interplay of Fe–Ni atom pairs embedded in nitrogen-doped carbon for bifunctional oxygen electrocatalysis**. *Nano Energy* 2020, **71**, 104597. https://www.sciencedirect.com/science/article/pii/S2211285520301555.

This work reports the fabrication of a cost-effective OER/ORR bifunctional catalyst by embedding atomic Fe–Ni dual metal pairs into N-doped hollow carbon spheres. The resultant catalyst shows an exceptional catalytic performance towards both OER and ORR, which is even comparable to that of noble metal-based benchmarks.

54. Luo F, Zhu J, Ma S, Li M, Xu R, Zhang Q, Yang Z, Qu K, Cai W, Chen Z: **Regulated coordination environment of Ni single atom catalyst toward high-efficiency oxygen electrocatalysis for rechargeable zinc-air batteries**. *Energy Storage Mater* 2021, **35**:723–730. https://www.sciencedirect.com/science/article/pii/S2405829720304694.

55. Yu D, Ma Y, Hu F, Lin C-C, Li L, Chen H-Y, Han X, Peng S: **Dual-sites coordination engineering of single atom catalysts for flexible metal–air batteries**. *Adv Energy Mater* 2021, **11**, 2101242, https://doi.org/10.1002/aenm.202101242.

56. ** Zhou X, Gao J, Hu Y, Jin Z, Hu K, Reddy KM, Yuan Q, Lin X, Qiu H-J: **Theoretically revealed and experimentally demonstrated synergistic electronic interaction of CoFe dual-metal sites on N-doped carbon for boosting both oxygen reduction and evolution reactions**. *Nano Lett* 2022, **22**:3392–3399, https://doi.org/10.1021/acs.nanolett.2c00658.

DFT calculations show that FeCo represents the best combination of two transition metal atoms from Fe, Co, and Ni supported in N-doped graphene for optimal bifunctional oxygen electrocatalysis. This is confirmed by experimental results.

57. Wan W, Zhao Y, Wei S, Triana CA, Li J, Arcifa A, Allen CS, Cao R, Patzke GR: **Mechanistic insight into the active centers of single/dual-atom Ni/Fe-based oxygen electrocatalysts**. *Nat*

Commun 2021, **12**:5589, https://doi.org/10.1038/s41467-021-25811-0.

58. Sun Z, Lin L, He J, Ding D, Wang T, Li J, Li M, Liu Y, Li Y, Yuan M, Huang B, *et al.*: **Regulating the spin state of FeIII enhances the magnetic effect of the molecular catalysis mechanism**. *J Am Chem Soc* 2022, **144**:8204–8213, https://doi.org/10.1021/jacs.2c01153.

59. Li J, Sougrati MT, Zitolo A, Ablett JM, Oğuz IC, Mineva T, Matanovic I, Atanassov P, Huang Y, Zenyuk I, Di Cicco A, *et al.*: **Identification of durable and non-durable FeNx sites in Fe–N–C materials for proton exchange membrane fuel cells**. *Nat. Catal.* 2020, **4**:10–19, https://doi.org/10.1038/s41929-020-00545-2.

60. Li XN, Cao CS, Hung SF, Lu YR, Cai WZ, Rykov AI, Miao S, Xi SB, Yang HB, Hu ZH, Wang JH, *et al.*: **Identification of the electronic and structural dynamics of catalytic centers in single-Fe-atom**. *Chem* 2020, **6**:3440–3454. https://www.sciencedirect.com/science/article/pii/S2451929420305830.

61. Liu K, Fu J, Lin Y, Luo T, Ni G, Li H, Lin Z, Liu M: **Insights into the activity of single-atom Fe-N-C catalysts for oxygen reduction reaction**. *Nat Commun* 2022, **13**:2075, https://doi.org/10.1038/s41467-022-29797-1.

62. Yang G, Zhu J, Yuan P, Hu Y, Qu G, Lu B-A, Xue X, Yin H, Cheng W, Cheng J, Xu W, *et al.*: **Regulating Fe-spin state by atomically dispersed Mn-N in Fe-N-C catalysts with high oxygen reduction activity**. *Nat Commun* 2021, **12**:1734, https://doi.org/10.1038/s41467-021-21919-5.

63. Li H, Wang J, Qi R, Hu Y, Zhang J, Zhao H, Zhang J, Zhao Y: **Enhanced Fe 3d delocalization and moderate spin polarization in FeNi atomic pairs for bifunctional ORR and OER electrocatalysis**. *Appl. Catal. B* 2021, **285**, 119778. https://www.sciencedirect.com/science/article/pii/S0926337320311954.

64. ** He T, Chen Y, Liu Q, Lu B, Song X, Liu H, Liu M, Liu Y-N, Zhang Y, Ouyang X, Chen S: **Theory-guided regulation of FeN_4 spin state by neighboring Cu atoms for enhanced oxygen reduction electrocatalysis in flexible metal-air batteries**. *Angew Chem Int Ed* 2022, **61**, e202201007. https://onlinelibrary.wiley.com/doi/abs/10.1002/anie.202201007.

This work shows a nearly linear correlation of the energy barriers of ORR with the Fe magnetic moment. When single Cu sites are incorporated into Fe–N–C aerogels, the Fe centers exhibit a reduced magnetic moment and markedly enhanced ORR activity within a wide pH range of 0–14.

65. Walling C: **Fenton's reagent revisited**. *Acc Chem Res* 1975, **8**: 125–131. https://pubs.acs.org/doi/pdf/10.1021/ar50088a003.

66. Liu S, Li C, Zachman MJ, Zeng Y, Yu H, Li B, Wang M, Braaten J, Liu J, Meyer HM, Lucero M, *et al.*: **Atomically dispersed iron sites with a nitrogen–carbon coating as highly active and durable oxygen reduction catalysts for fuel cells**. *Nat Energy* 2022, https://doi.org/10.1038/s41560-022-01062-1.

67. Chen Y, He T, Liu Q, Hu Y, Gu H, Deng L, Liu H, Liu Y, Liu Y-N, Zhang Y, Chen S, *et al.*: **Highly durable iron single-atom catalysts for low-temperature zinc-air batteries by electronic regulation of adjacent iron nanoclusters**. *Appl. Catal. B* 2023, **323**, 122163. https://www.sciencedirect.com/science/article/pii/S0926337322011043.